

SUPPLEMENTARY INFORMATION

1. Periodicity modes

An *in situ* characterization of the periodicity of the grating was performed through the scattering of the diffracted beams in transmission geometry. The strongly diffracted beams act as input beams for subsequent scattering in the glass substrate by the bulk longitudinal and transverse phonons. Their frequency shift is described by

$$f(k) = \frac{c_{glass}}{2\pi} \sqrt{G^2 + k^2 \pm 2Gksin\varphi} \quad (\text{Eq. S1})$$

Here $G = 2\pi/a$ is the reciprocal lattice constant, φ is the relative angle between the probing wave vector \mathbf{q} and the nanowalls (Figure 5 inset) and c_{glass} is the sound velocity in the glass substrate. Equation 1 is obtained from $f = c_{glass}q/2\pi$, with $q^2 = q_x^2 + q_y^2$, and $q_y = k \pm G$, due to the momentum conservation.¹ For propagation along the nanowalls ($\varphi = 0$), there are two branches (p_L and p_T in Figure 2c) dependent on substrate sound velocity, either the longitudinal or the transverse (Table 2). If q has a y -component ($\varphi \neq 0$) with an orientation as small as 1° , each “periodicity peak” in the BLS spectrum splits into a doublet; thus there are four branches in the dispersion plot. The sensitivity of the spectrum to the nanowall orientation in the scattering plane allows a precise control on the q -direction. Representation of the experimental points by Supplementary Eq. 1 (solid lines in Figure 2c) using fixed the known values of the two glass sound velocities yields the lattice parameter a .

2. Band sorting method

The calculation of the dispersion curves from which the densities of states and Brillouin scattering spectra can be deduced based on the finite element method (FEM, see Methods). Since the material of nanowalls have very different acoustic impedance ($Z = c\rho$) than the substrate, we shall be mostly interested in the modes below the sound lines of the glass substrate (red lines in Figure S1a) which are highly confined inside the nanowalls and cannot penetrate into the substrate. Still, due to the finite size of the nanowalls and nanolines, there are a great number of dispersion curves below the glass sound lines. One can make a selection of the modes for which the displacement field is mainly composed of u_x and u_y components. This selection is based on a band sorting method by means of the following relation

$$P_{xy} = \frac{\iiint_{Nanowalls} (|u_x|^2 + |u_y|^2) dv}{\iiint_{unitcell} (|u_x|^2 + |u_y|^2 + |u_z|^2) dv} \quad (\text{Eq. S2})$$

This relation means that the mode which have mainly u_x and u_y components display a P_{xy} close to 1, whereas the modes with u_z component have P_{xy} close to 0. Figure S1b shows the dispersion branches

that satisfy to the condition $P_{xy} \geq 0.8$. One can recognize a similarity between these modes and those of an infinite plate of equal thickness as the nanowall (Figure S2a). Therefore we call them S_n and A_n like (n is an integer) for the modes whose displacement fields are respectively symmetric and antisymmetric with respect to the mid-plane of the plate.

3. Morphological effects

To examine whether morphological changes of the nanolines and nanowalls relate to the observed change of the elastic parameters, we consider the effect of the grating wall shape. Deviation from the theoretical rectangular shape is feasible in the soft matter. We consider two deviations from the ideal straight rectangular shape: (i) round top and round grafting of the nanolines to the substrate (Figure S5) and (ii) trapezoidal nanowalls being narrower on the top than at the bottom (Figure S6). The BLS intensities and the dispersion relation are not significantly affected by including a small rounding either on the top (Figure S6b) or at the bottom (Figure S6c) of the nanowall structure.² The second shape defect (trapezoidal) can relate to the sinusoidal profile of the interference light pattern. Only above a critical light intensity the oligomers will be crosslinked; hence the bottom of the nanowalls should have larger crosslinking area than the top, leading to a broader bottom of the nanowalls. The computed BLS intensity-dispersion relation of a trapezoidal nanowall can be understood as the superposition of the dispersions by a nanowall with thickness in a range 100-250 nm. The S_0 and S_1 -like bands are broad because the phase-matching frequency sweeps the acoustic dispersion curve as the width of the nanowall increases. That creates an apparent blue-shift of the S-like modes (Figure S6a). The increase of the sound velocities, in general, causes a blue-shift of the modes (Figure S3) but it does not suffice to completely capture the blue shift of the resolved acoustic branches. More specifically, the S_0 -like mode is sensitive to c_T as well as the S_1 -like mode but at higher wave vectors (Figure S3). In contrast, the increase of c_L mostly produces a blue shift of only S_1 and S_2 -like modes. The trapezoidal shape, together with the slight increase in velocities is necessary to completely describe the experimental dispersion. In conclusion, the phononic dispersion of nanowalls is very sensitive to variations in the wall thickness, but not variations of their edges shape.

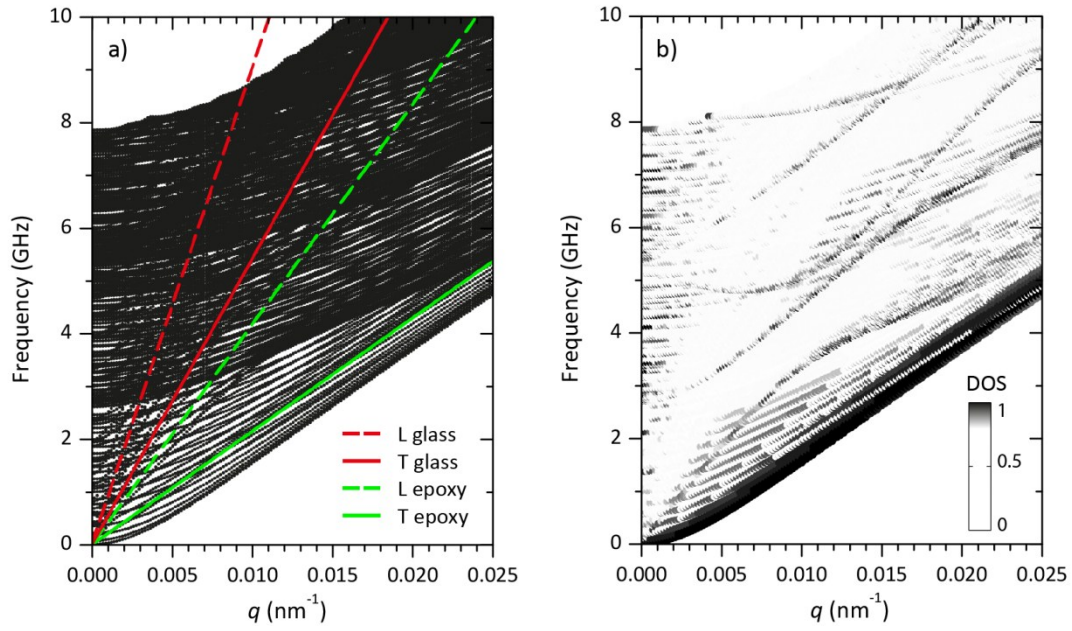


Figure S1: (a) Full dispersion curves of nanowalls calculated for their 300 first eigenfrequencies. (b) Dispersion curves of the modes with mainly u_x and u_y components ($P_{xy} \geq 0.8$).

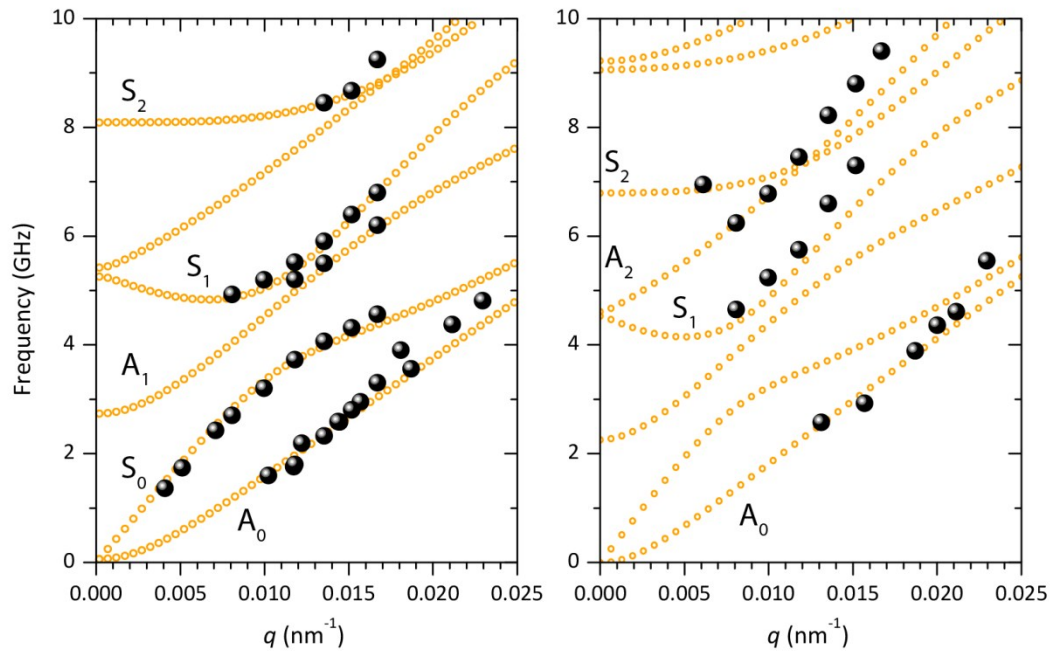


Figure S2: Lamb plate theoretical dispersion plot (orange open circles) and experimental dispersion (black spheres) for (a) high aspect ratio nanowalls and (b) short aspect ratio nanolines. The experimental points have been acquired in both T and BS geometry.

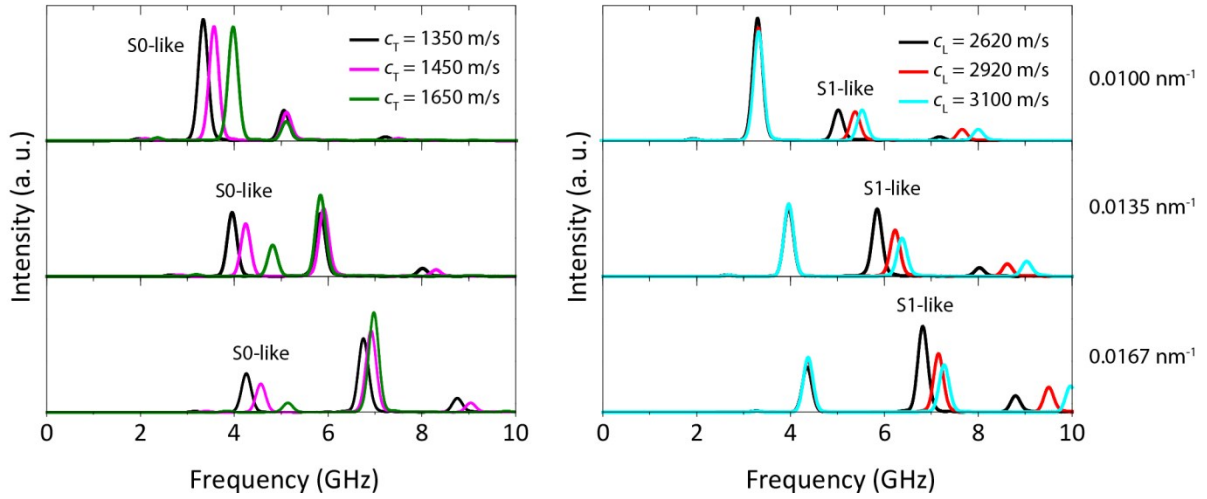


Figure S3: (a-b) Effect of (a) c_T and (b) c_L in high AR nanowalls BLS intensity. S0-like mode is sensitive mainly to c_T while S1-like mode is sensitive to c_L and to c_T in lesser degree. The sound velocity has been fixed to $c_L = 2620$ m/s in (a) and $c_T = 1350$ m/s in (b).

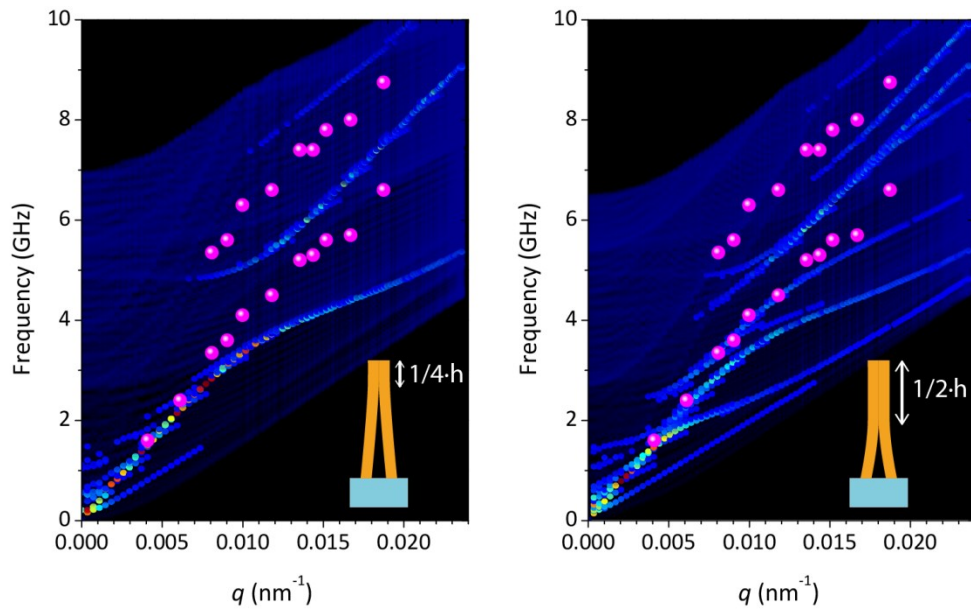


Figure S4: Effect of the contact between high aspect ratio nanowalls in the VV BLS intensity: (a) small contact area, nanowalls touch about $1/4$ of their height; (b) large contact area, nanowalls touch about $1/2$ of their height. The bands of greater intensity in (b) correspond to the Lamb modes of a plate of $2w$ width.

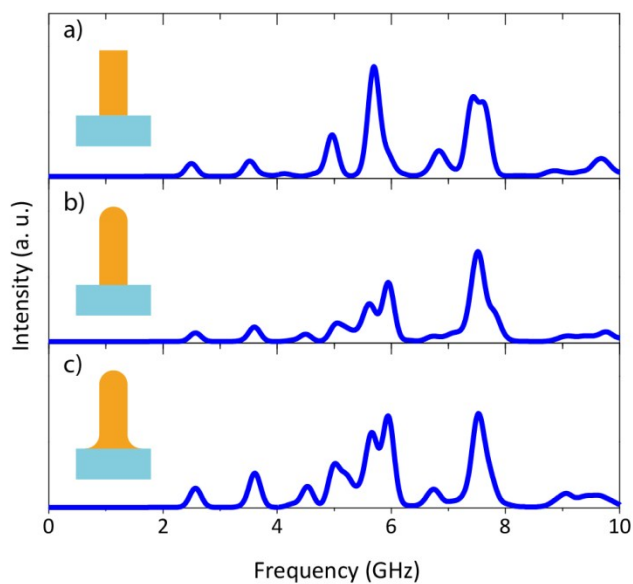


Figure S5: Theoretical BLS spectra at $q = 0.0118 \text{ nm}^{-1}$ as a function of the nanoline section shape.

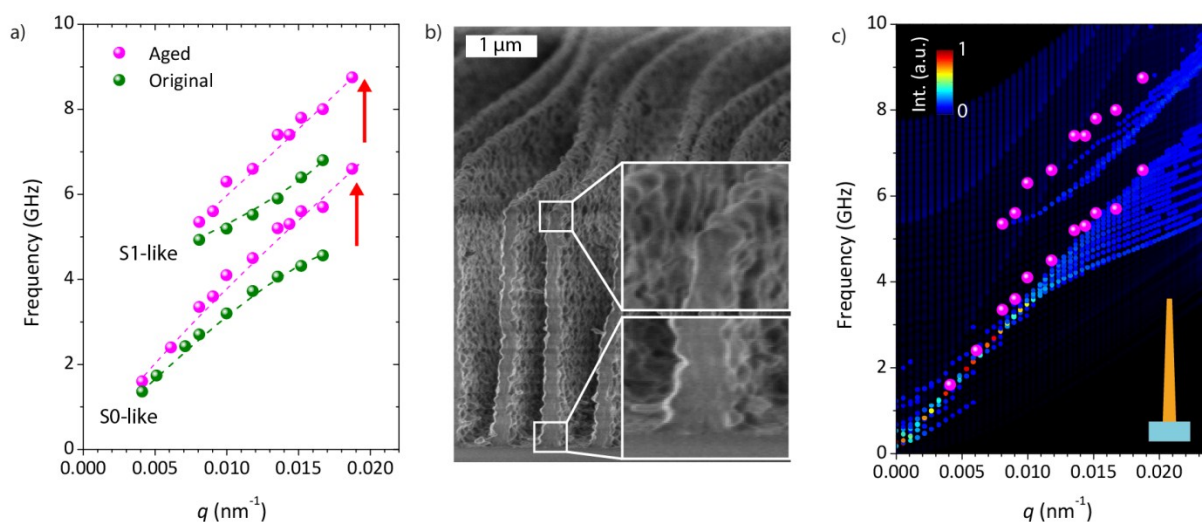


Figure S6: (a) Experimental dispersion plot (VV polarization) of trapezoidal aged nanowalls (pink) is blue-shifted respect to the original (green). (b) Cross section SEM micrograph displays the distinct width at the base (bottom inset) and the top (upper inset) of the nanowalls. (c) Dispersion relation colored according to the VV BLS intensity.

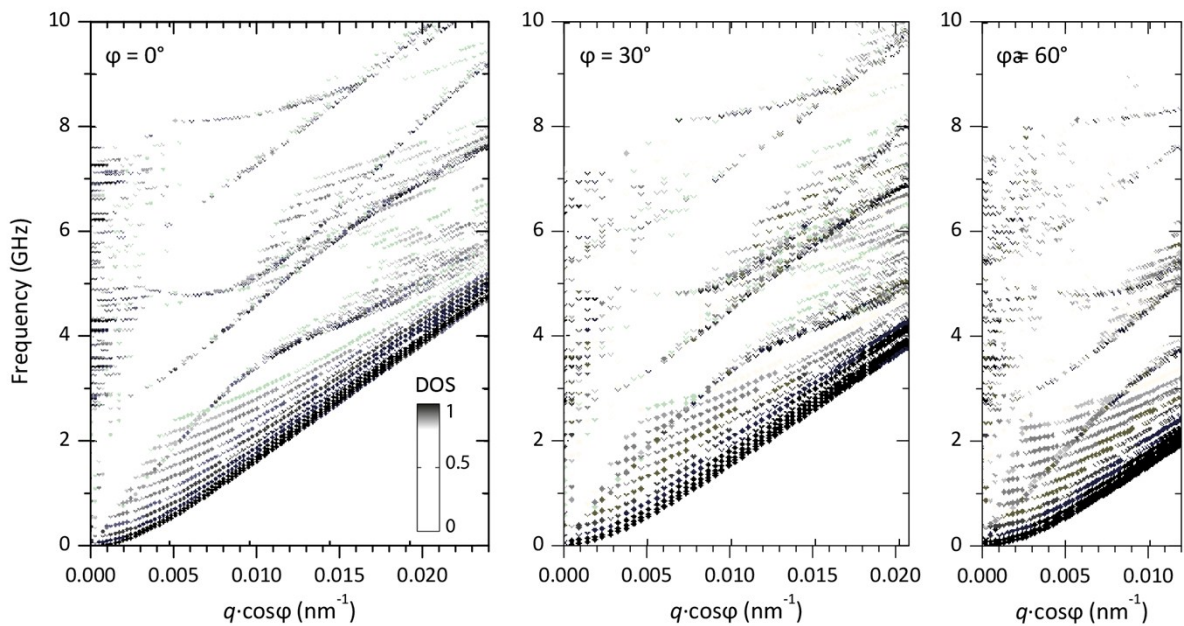


Figure S7: Normalized density of states (DOS) for long nanowalls, as a function of the projected q along the nanowalls, for three different orientations φ .

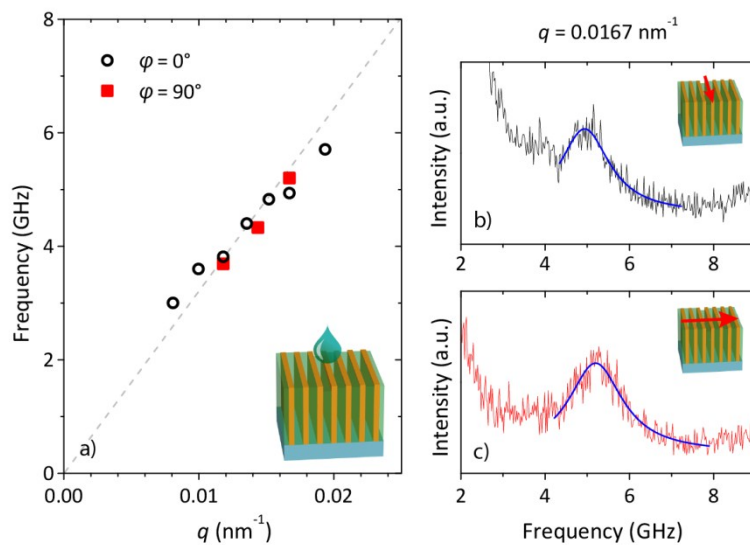


Figure S8: (a) Experimental dispersion relation measured with probing q along ($\varphi = 0^\circ$) and perpendicular ($\varphi = 90^\circ$) to the nanowalls of the grating filled with *Cargille* liquid. The dashed line is a guide for the eye. (b-c) VV spectra at 0.0167 nm^{-1} (b) along and (c) across the nanowalls.

■ SUPPLEMENTARY REFERENCES

1. Urbas, A. M.; Thomas, E. L.; Kriegs, H.; Fytas, G.; Penciu, R. S.; Economou, L. N., *Phys. Rev. Lett.* **2003**, *90* (10), 108302.
2. Johnson, W. L.; Kim, S. A.; Geiss, R.; Flannery, C. M.; Soles, C. L.; Wang, C.; Stafford, C. M.; Wu, W. L.; Torres, J. M.; Vogt, B. D.; Heyliger, P. R., *Nanotechnology* **2010**, *21* (7), 75703.